Ocean Engineering 307 (2024) 118215

Contents lists available at ScienceDirect

Ocean Engineering

journal homepage: www.elsevier.com/locate/oceaneng

# Experiment design for model basin tests with a remotely operated vehicle

Elías Revestido Herrero *, Jose Ramon Llata, Jose Joaquin Sainz, Francisco J. Velasco, Luciano Alonso Renteria

*Departamento de Tecnología Electrónica, Ingeniería de Sistemas y Automática, Universidad de Cantabria, Av. de los Castros s/n- 39005, Santander (Cantabria), Spain*

ARTICLE INFO

*Keywords:*
Experiment design
Parameter sensitivity
Maneuvering models
Mini max

ABSTRACT

In this paper, we propose an experiment design methodology for model basin tests with a remotely operated vehicle (ROV) to estimate model parameters. We propose and compare two different optimization problems based on a parameter sensitivity approach for the modification of the standard inputs used in model basin tests. A procedure is established for the design of experiments for model basin tests and it is applied to the data acquired in the Centro de Experiencias Hidrodinámicas del Pardo INTA/CEHIPAR model basin tests. Through the Monte Carlo study, the statistical properties of the estimated parameters are quantified to verify the improvement when the designed excitation signal is applied.

There has been a significant increase in the use of autonomous underwater vehicles in different types of tasks over the past few decades (Schjlberg and Utne, 2015; Fay et al., 2019). These tasks involve high-risk operations such as exploration of underwater areas, performing survey trajectories harvesting data to build bathymetric maps, and inspections of underwater structures or elements (e.g., pipelines or underwater cables) which require complex motion control methods and localization methods. Recent advances in AUVs' performance have led to them playing an important role in the cited operations, relaying ROVs and manned submersibles to second place. However, intervention applications, where the system manipulates the environment, are still mainly performed by ROVs due to the complexity of the task. In open-loop remote operation, the user must perform accurate maneuvers while dealing with currents, waves, and the effects of the ROV's tether. Additionally, for some specific classes of ROVs (I or II) (Robert L. Wernli, 2014; Capocci et al., 2017), kinematic constraints due to under-actuation can be an additional hindrance to teleoperation performance. Therefore, a control scheme applied in a fully or semi-autonomous ROV is likely the best solution for these underwater applications.

As far as motion control applications for ROVs are concerned, it is common practice to obtain non-linear maneuvering models from open waters or model basin tests when developing a suitable control system. The accuracy of the model is essential for motion control and navigation applications, particularly when model-based control methods are used. In the literature, there is a wide variety of contributions where different types of system identification techniques are applied to obtain the hydrodynamical parameters of the cited models for a particular set of fixed input signals. These references are not reviewed in this paper, since we focus our attention on experiment design methods, which also have a significant impact on the accuracy of the obtained maneuvering model. In this sense, it is common practice to use random excitation signals (Barker et al., 2006; Braun et al., 2001; Rojas et al., 2012) to excite the dynamics of the model to be identified. However, these signals have the disadvantage, that the trajectory to be described by the vehicle with the random signal can be outside the restricted area in which the tests are performed, which is the case of the estimation of maneuvering model parameters with model basin tests, which is the aim of the present paper.

In the particular case of parameter estimation of non-linear maneuvering models, some references are found (Blanke and Knudsen, 1999, 2006; Herrero et al., 2012), in which it is used a parameter sensitivity approach for the design of experiments. These authors, propose the design of experiments based on standard maneuvers for ships and also an alternative excitation signal to the standard zig-zag maneuver. The experiment design for parameter estimation based on parameter sensitivity theory presents features which are highly appropriate for obtaining maneuvering models: it presents a greater independence of noise, due to the geometrical interpretation considered in the cited

* Corresponding author.
*E-mail addresses:* revestidoe@unican.es (E.R. Herrero), llataj@unican.es (J.R. Llata), josejoaquin.sainz@unican.es (J.J. Sainz), velascof@unican.es (F.J. Velasco), luciano.alonso@unican.es (L.A. Renteria).
*URLs:* https://www.marinelabcantabria.unican.es (E.R. Herrero), https://www.marinelabcantabria.unican.es (J.R. Llata), https://www.marinelabcantabria.unican.es (F.J. Velasco).

https://doi.org/10.1016/j.oceaneng.2024.118215
Received 27 July 2023; Received in revised form 16 April 2024; Accepted 16 May 2024
Available online 25 May 2024

theory. These characteristics have certain advantages over other known criteria for experiment design previously reported in the literature, specifically the design of optimal experiments; such as the covariance information matrix of the estimates, covariance information matrix, or the Fisher information matrix (Goodwin and Payne, 1977; Ljung, 1987; Söderström and Stoica, 1994). These last approaches have the following drawbacks: they are based on certain assumptions that are difficult to implement in practice, are incompatible with physical knowledge, and apply only to parameter estimates of discrete-time linear models.

More recent works regarding the experiment design of non-linear systems combine graph methods with particle filters as in Valenzuela et al. (2014), which extends the input design methods initially proposed in Gopaluni et al. (2009) and Valenzuela et al. (2013). In the work of Bombois et al. (2021), a robust optimal identification experiment design methodology is developed for multisine excitation signals, which can be very convenient for the present paper taking into consideration that the standard inputs used in model basin tests present a multisine form for the sway, heave and yaw degrees of freedom (DOF) (e.g. see Fig. 2). However, the cited work is developed only for linear time-invariant (LTI) systems, as in Rojas et al. (2012) where the robustness of experiment design is treated for LTI systems. The work of Denisov et al. (2019) also includes robust estimation by means of a procedure of active identification, which is resistant to the appearance of anomalous observations and optimal design of input signals for models of non-stationary linear discrete systems. Dirkx et al. (2023) also tackles the robust design problem by formulating an infinite-dimensional min–max optimization problem via the S-lemma in an iterative approximation scheme for multi-variable systems. In the contribution of McMichael and Blakley (2022) simplified Algorithms for Adaptive Experiment Design are established with good results, but it has a drawback in that it is impractical to use in certain applications, such as that of the present paper in which the input signals to be designed is limited in amplitude and frequency, apart from the restrictions due to security aspects in the performance of the test. Furthermore, while these simplified algorithms make sense in on-line estimation, in the off-line applications of this paper they are not so relevant. In addition, in the work of Fredrik Ljungberg and Tervo (2023), experiment design for marine vessels is explored based on a dictionary-based approach, which is tailored to an instrumental variable (IV) estimator with zero-mean instruments.

For other types of applications, the experiment design for parameter estimation of equivalent-circuit battery models is investigated both quantitatively and qualitatively, see Beelen et al. (2018). In Gottu Mukkula and Paulen (2019), a model-based optimal experiment design (OED) of non-linear systems is studied. This work represents a methodology for optimizing the geometry of the parametric joint-confidence regions (CRs) with interesting levels of accuracy for simple models. In this paper, it is used to consider a case study with a couple of parameters. For complex models with more parameters the configuration of the CR might be highly complex or even intractable. In like manner, in the work of Denis-Vidal et al. (2019), an optimal experiment design approach is proposed for parameter estimation in a bounded-error context with some similarities to the one of Gottu Mukkula and Paulen (2019), which is robust to the actual value of the vector of parameters. Du et al. (2019) propose a new approach for on-line parameter estimation in power systems based on optimal experimental design using multiple measurement snapshots. Regarding air-crafts, in Alabsi and Fields (2019) an optimization problem that is based on information matrices is solved for finding the optimal robot configurations for the identification experiment in the frequency domain. For industrial robots, Zimmermann et al. (2023) develop an experimental work, in which experiment design is improved with respect to previous works by a proposed method in terms of efficiency and parameter accuracy. In the cited paper, a significantly shorter time is used for conducting data collection experiments and the average standard deviation of the parameter estimate is reduced.

In this paper, we propose an experiment design methodology for model basin tests with an ROV to estimate non-linear maneuvering model parameters. We formulate and compare two different optimization problems based on a parameter sensitivity approach for the modification of the standard inputs used in model basin tests. It is established as a procedure for the design of experiments for model basin tests and it is applied to the data acquired in the Centro de Experiencias Hidrodinámicas del Pardo INTA/CEHIPAR model basin. Through a Monte Carlo study, the statistical properties of the estimated parameters are quantified to verify the improvement when the designed excitation signals are applied.

This paper is organized as follows. Section 2 discusses the non-linear maneuvering models. Sections 3 and 4 develop the model basin trials carried out in the INTA/CEHIPAR and the experiment design, respectively.Section 4 discusses a study case and Section 5 presents the conclusions.

## 1. Non linear maneuvering model

To describe the ROV motion which is the object of study of this work (see Appendix), three translational coordinates are needed and another one for the yaw angle. Two coordinate systems are used to study the ROV movement: one coordinate is fixed to the vehicle and is used to define its translational and rotational movements and another one is located on Earth (NED-frame) to describe its position and orientation. The NED-frame and the body-fixed frame affixed to the vehicle center of gravity (CG) (Fossen, 2011; Soylu et al., 2016).

The non-linear maneuvering model can be expressed in the following form (Fossen, 2002):

$$\mathbf{M}\dot{\nu} + \mathbf{C}(\nu)\nu + \mathbf{D}(\nu)\nu + \mathbf{g}(\eta) = \tau, \tag{1}$$

$$\dot{\eta} = \mathbf{J}(\eta)\nu \tag{2}$$

$$y_s = \nu + w, \tag{3}$$

where $\eta = [x, y, z, \psi]^T$ is the position and yaw angle vector, $\nu = [u, v, w, r]^T$ are the linear speeds and yaw angular speed, $\tau = [X, Y, Z, N]^T$ are the forces and moments and $\omega$ is the measurement noise. $\mathbf{M}$ is the rigid body and added mass matrix, $\mathbf{C}(\nu)\nu$ is the Coriolis term, $\mathbf{g}(\eta)$ is the restore matrix and $\mathbf{J}(\eta)$ is the rotation matrix and $\mathbf{D}(\nu)\nu$ represents the hydrodynamic damping forces that are a combination of linear and non linear damping. It must be noted that the thruster layout on the ROV object of study of this work (see Appendix), cannot actively control the roll and pitch motion of the vehicle. That is why we consider only four degrees of freedom (DOF), assuming that the pitch and roll motions are small. Since the roll and pitch angles are small the kinematic relationship between the speed $\nu$ in the body-fixed coordinate system and the position $\eta$ in the NED (North East Down) coordinate system is given by:

$$\mathbf{J}(\eta) = \begin{bmatrix} cos(\psi) & cos(\psi) - sin(\psi) & 0 & 0 \\ sin(\psi) & cos(\psi) & 0 & 0 \\ 0 & 0 & 1 & 0 \\ 0 & 0 & 0 & 1 \end{bmatrix} \tag{4}$$

The rest of the matrices for the 4 DOF model of Eq. (1) are the following:

The rigid body and added mass matrices, $\mathbf{M}= M_{RB} + M_A$.

$$M_{RB} = \begin{bmatrix} m & 0 & 0 & 0 \\ 0 & m & 0 & 0 \\ 0 & 0 & m & 0 \\ 0 & 0 & 0 & I_r \end{bmatrix} \tag{5}$$

where $m$ is the mass of the vehicle, $I_z$ is the inertia moment in the yaw degree of freedom.

$$M_A = \begin{bmatrix} X_{\dot{u}} & 0 & 0 & 0 \\ 0 & Y_{\dot{v}} & 0 & 0 \\ 0 & 0 & Z_{\dot{w}} & 0 \\ 0 & 0 & 0 & I_{\dot{r}} \end{bmatrix} \tag{6}$$

In this article, it is considered that the ROV operates at depths below the area affected by the movement induced by the waves. Therefore, it is considered that the coefficients of the added mass matrix are constant: for more details on this aspect and on operating conditions see Pérez and Fossen (2006), Fossen (2011).

The Coriolis matrix $\mathbf{C}(v)$

$$\mathbf{C}(v) = \begin{bmatrix} 0 & 0 & 0 & -mv \\ 0 & 0 & 0 & mu \\ 0 & 0 & 0 & 0 \\ mv & -mu & 0 & 0 \end{bmatrix} \tag{7}$$

The damping matrices $\mathbf{D}(v)v = D_l(v)v + D_{nl}(v)v$

$$D_l(v) = \begin{bmatrix} X_u & 0 & 0 & 0 \\ 0 & Y_v & 0 & 0 \\ 0 & 0 & Z_w & 0 \\ 0 & 0 & 0 & N_r \end{bmatrix} \tag{8}$$

$$D_{nl}(v) = \begin{bmatrix} X_{u|u|}|u| & 0 & 0 & 0 \\ 0 & Y_{v|v|}|v| & 0 & 0 \\ 0 & 0 & Z_{w|w|}|w| & 0 \\ 0 & 0 & 0 & N_{r|r|}|r| \end{bmatrix} \tag{9}$$

where $D_l(v)$ includes the linear damping terms and $D_{nl}(v)$ the non-linear ones.

Note that the components of the restoring forces and moments vector $\mathbf{g}(\eta)$ are considered 0, see Shen et al. (2017).

## 2. Model basin tests

This section sums up the tests that were performed at the INTA/CEHIPAR for the parameter estimation of the mathematical model defined in Eq. (1). For this purpose, a commercial ROV was used, see Appendix for more details in the experimental set up and the ROV. Fig. 1 shows two different assemblies of the vehicle in the calm water channel of the INTA/CEHIPAR. The vehicle is turned 90 degrees depending on the degree of freedom that it is going to be tested, see right and left parts of Fig. 1. The tests consisted of making different controlled movements of the ROV moving through the fluid by means of two computer-controlled linear actuators mounted on the towing carriage, see Table 1 for the conditions and the parameters estimated in each test. In each actuator, a 6-component dynamo-meter was mounted and a ball joint allowing rotation in sway. In the different tests, the transverse and vertical accelerations were measured with 2 accelerometers, one at each end of each actuator. The total forces and the total yaw moment were calculated off-line in the center of gravity of the vehicle with the measurements of the cited instrumentation by means of an inertial table, see Appendix. Furthermore, the total movement of the ROV in the center of gravity was calculated based on the displacement of the linear actuators, thus enabling the input signals applied in each model basin test to be calculated, see Fig. 2. These typical input signals are modified by the experiment designed procedure proposed in the next section.

The tests performed were as follows:

- Longitudinal drag and acceleration at 3 speeds: the vehicle is dragged at different speeds and the vector of parameters $\hat{\theta}_1$ is estimated. By considering the conditions of this test ($v = w = p = r = \phi = \theta = \psi = 0$) the result from Eq. (1) for surge is:

$$X = X_u + X_{u|u|}u|u| + (-m + X_{\dot{u}})\dot{u} \tag{10}$$

- Dynamic heave at one frequency and three amplitudes (zero speed and nominal sailing): the vector of parameters $\hat{\theta}_2$. Is estimated by considering the conditions of this test ($v = p = r = \phi = \theta = \psi = 0$). The result from Eq. (1) for heave is::

$$Z = (-m + Z_{\dot{w}})\dot{w} + Z_{w|w|}w|w| + Z_w w \tag{11}$$

**Fig. 1.** ROV assemblies in the INTA/CEHIPAR calm water channel, right upright position and left ROV turned 90 degrees.

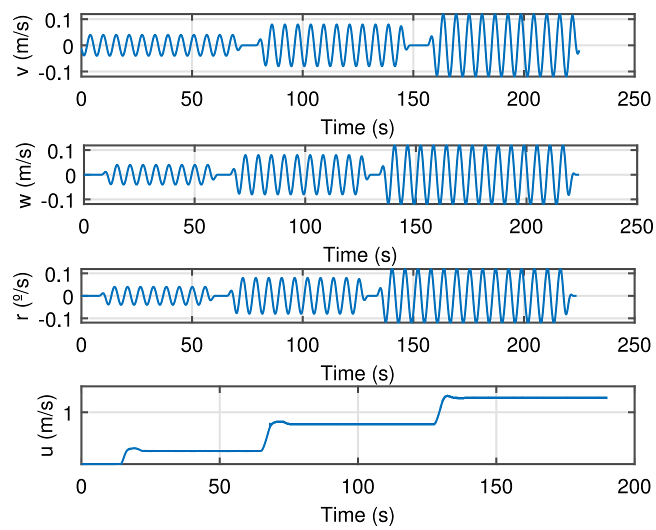


**Fig. 2.** Standard model basin input data obtained from the INTA/CEHIPAR tests.

- Static Heave at 3 angles (nominal sailing speed) (Fig. 1, right assembly): See procedure and conditions for static tests (Committee, 2014).
- Dynamic Sway at one frequency and three amplitudes (zero speed and nominal sailing): the vectors of parameters $\hat{\theta}_3$. Is estimated by considering the conditions of this test ($w = p = r = \phi = \theta = \psi = 0$). The resulting equation for the sway force is:

$$Y = (-m + Y_{\dot{v}})\dot{v} + Y_v v + Y_{|v|v}|v|v \tag{12}$$

- Static Sway at 3 angles (nominal sailing speed): See procedure and conditions for static tests (Committee, 2014).
- Dynamic Yaw at one frequency and three amplitudes (zero speed and nominal sailing): the vector of parameters $\hat{\theta}_4$ is estimated. See pitching motion conditions ($v = w = p = q = \phi = \theta = 0$) (Lee et al., 2011) and the resultant from Eq. (1) for the yaw moment is:

$$N = (-I_{zz} + N_{\dot{r}})\dot{r} + (N_r - mx_G u)r + N_{|r|r}|r|r \tag{13}$$

- Static Yaw at 3 angles (nominal sailing speed): See procedure and conditions for static tests (Committee, 2014).

For more details on this type of tests see Revestido Herrero et al. (2018), Phillips et al. (2007).

## 3. Experiment design

We propose two different optimization problems for model basin experiment design with the aim of maneuvering models (Eq. (1))

**Table 1**
Summary table of the tests carried out at the INTA/CEHIPAR facilities.

| Test | Estimated parameters $\hat{\theta}_{j,i}$ | Speeds (Kn) | Amplitude ROV CG Motion (mm) | Assembly Fig. 1 |
|---|---|---|---|---|
| Resistance and longitudinal acceleration | $\hat{\theta}_1 = [X_{\dot{u}}, X_u, X_{u\|u\|}]^T$ | 0.5, 1.5, 2.5 | | Left |
| Dynamic Heave | $\hat{\theta}_2 = [Z_{\dot{w}}, Z_w, Z_{w\|w\|}]^T$ | 0,2 | 40, 80, 120 | Left |
| Dynamic Sway | $\hat{\theta}_3 = [Y_{\dot{v}}, Y_v, Y_{v\|v\|}]^T$ | 0,2 | 40, 80, 120 | right |
| Dynamic Yaw | $\hat{\theta}_4 = [N_{\dot{r}}, N_r, N_{r\|r\|}]^T$ | 0,2 | 50, 100, 150 | right |

parameter estimation:

$$\min_{\theta_{j,i}} \{R(\theta_{j,i}, \Theta_{j,i})\} \equiv \left\{ lb_{j,i} \le \theta_{j,i} \le ub_{j,i} \right. \tag{14}$$

$$\min_{\theta_{j,i}} \max_{k} \left\{ R_j(\theta_{j,i}, \Theta_{j,i})\ R_{j,i}(\theta_{j,i}, \Theta_{j,i})\ \frac{1}{S_{jmin}(\theta_{j,i}, \Theta_{j,i})}\ \frac{1}{S_{j,imin}(\theta_{j,i}, \Theta_{j,i})} \right\} \equiv \left\{ lb_{j,i} \le \theta_{j,i} \le ub_{j,i} \right. \tag{15}$$

where $R_j(\theta_{j,i}, \Theta_{j,i})$ is the sensitivity ratio of the $j$th DOF, $R_{j,i}(\theta_{j,i}, \Theta_{j,i})$ is the sensitivity ratio of the $i$th input parameter of the $j$th DOF, $S_{jmin}(\theta_{j,i}, \Theta_{j,i})$ is the minimum sensitivity of the $j$th DOF, $S_{j,imin}(\theta_{j,i}, \Theta_{j,i})$ is the sensitivity ratio of the $i$th input parameter of the $j$th DOF, $\theta_{j,i}$ is the $i$th input parameter of the $j$th DOF, $\Theta_{j,i}$ is the $i$th maneuvering model parameter of Eq. (1) of the $j$th DOF, $lb_{j,i}$ is the lower bound of the $i$th element of $\theta_{j,i}$ for the $j$th DOF and $ub_{j,i}$ is the upper bound of the $i$th element of $\theta_{j,i}$ for the $j$th DOF. Note that the $j$ refers to the DOFs of the model defined in Eq. (1), being $j = 1$ the surge DOF, $j = 2$ the sway DOF, $j = 3$ the heave DOF and $j = 4$ the yaw DOF. The sub-index $i$ refers to the $i$th parameter of the input signal to be optimized and the sub-index $k$ to $k$th element of the minimax problem.

Note that Eq. (16) involves a single parameter sensitivity calculation, making it computationally more efficient compared to Eq. (17), which requires multiple sensitivity calculations. Consequently, Eq. (16) is expected to be computationally cheaper than Eq. (17).

The experiment design proposed in this paper modifies the standard input signals conventionally used in model basin tests, see Fig. 2 for the standard input signals used in the INTA/CEHIPAR installations. More specifically, standard multisine input signals for the sway, heave, and yaw DOFs are designed by optimizing input parameters corresponding to three different amplitudes of cited multisine input, and for the surge DOF input signal, three parameters relative to the final value of surge speeds are designed.

The input to be designed for the surge DOFs is:

$$u \equiv \begin{cases} \frac{\theta_{j=1,i=1} \cdot w_n^2}{s^2 + 2\delta w_n s + w_n^2} & t_0 \le t \le t_1 \\ 0 & t \ge t_1 \\ \frac{\theta_{j=1,i=2} \cdot w_n^2}{s^2 + 2\delta w_n s + w_n^2} & t_1 \le t \le t_2 \\ 0 & t \ge t_2 \\ \frac{\theta_{j=1,i=3} \cdot w_n^2}{s^2 + 2\delta w_n s + w_n^2} & t_2 \le t \le t_3 \end{cases} \tag{16}$$

where $\delta$ is the damping ratio, $w_n$ is the undamped natural angular frequency, $t_0$ the initial instant of time, $t_3$ the final instant of time and $t_1, t_2$ intermediate instants of time, being $t_0 < t_1 < t_2 < t_3$. Note that it is chosen the kind of spectrum indicated in Eq. (16) very close to the spectrum of the input data acquired in the INTA/CEHIPAR installations, see Fig. 2 (The reader is referred to graph corresponding to the $u$ variable which presents a second-order system behavior).

The inputs to be designed for the sway, heave, and yaw are respectively:

$$v \equiv \begin{cases} \theta_{j=2,i=1} \cdot sin(wt) & t_0 \le t \le t_1 \\ 0 & t \ge t_1 \\ \theta_{j=2,i=2} \cdot sin(wt) & t_1 \le t \le t_2 \\ 0 & t \ge t_2 \\ \theta_{j=2,i=3} \cdot sin(wt) & t_2 \le t \le t_3 \end{cases} \tag{17}$$

$$w \equiv \begin{cases} \theta_{j=3,i=1} \cdot sin(wt) & t_0 \le t \le t_1 \\ 0 & t \ge t_1 \\ \theta_{j=3,i=2} \cdot sin(wt) & t_1 \le t \le t_2 \\ 0 & t \ge t_2 \\ \theta_{j=3,i=3} \cdot sin(wt) & t_2 \le t \le t_3 \end{cases} \tag{18}$$

$$r \equiv \begin{cases} \theta_{j=4,i=1} \cdot sin(wt) & t_0 \le t \le t_1 \\ 0 & t \ge t_1 \\ \theta_{j=4,i=2} \cdot sin(wt) & t_1 \le t \le t_2 \\ 0 & t \ge t_2 \\ \theta_{j=4,i=3} \cdot sin(wt) & t_2 \le t \le t_3 \end{cases} \tag{19}$$

where $w$ is the frequency of the sinusoidal function, $t_0$ the initial instant of time, $t_3$ the final instant of time and $t_1, t_2$ intermediate instants of time, being $t_0 < t_1 < t_2 < t_3$.

In Eqs. (16) to (19), the periods $t_1$, $t_2$, and $t_3$ were chosen to match those of the data collected in the INTA/CEHIPAR installations, as shown in Fig. 2. Specifically, $t_1$ corresponds to the first change in amplitude, $t_2$ to the second change in amplitude, and $t_3$ to the final moment in time. This approach ensures that the experiment design procedure starts with input signals that closely resemble the model basin ones, allowing for a comparison between the results obtained and the optimized ones. Note that the inputs of Eqs. (16) to (19), for the experiment design procedure proposed in this section, are specifically intended for the dynamic tests indicated in the previous section.

The sensitivity metrics used in the optimization problems defined above are based on parameter sensitivity theory (Blanke and Knudsen, 1999, 2006; Herrero et al., 2012), and their calculus are applied for the specific case of the maneuvering model of Eq. (1) as follows.

The sensitivity ratio for each DOF is defined by,

$$R_j(\theta_{j,i}, \Theta_{j,i}) = \frac{S_{jmax}}{S_{jmin}} = \frac{\sqrt{\lambda_{jmax}}}{\sqrt{\lambda_{jmin}}}, \tag{20}$$

$$\lambda_{j,i} = \{H_{dr}(\Theta_{j,i})\}_{ii} \tag{21}$$

where $S_{jmin}$ is the minimum sensitivity of the $j$th DOF, $S_{jmax}$ is the maximum sensitivity of the $j$th DOF and $\lambda$ denotes the eigenvalues of $H_{dr}$, which is calculated by doing

$$H_{dr}(\Theta_{j,i}) = T_r^T H_r(\Theta_{j,i}) T_r \tag{22}$$

$T_r$ being an orthogonal transformation matrix containing the eigenvectors of $H_r$ as columns.

The parameter $H_r$ is obtained by,

$$\theta_r = L^{-1}\Theta_{j,i}, L = diag(\hat{\Theta}_{j,i}) \tag{23}$$

$$H_r(\Theta_{j,i}) = L^T H(\hat{\Theta}_{j,i}) L \tag{24}$$

where $\hat{\Theta}_{j,i}$ is a local estimate of the parameters indicated in Eq. (1) around the optimal estimate. As the values of each of the maneuvering parameters indicated in Eq. (1) can be very different from each other, it is convenient to use relative sensitivities as it is done in Eq. (23).

The matrix Hessian $H(\hat{\Theta}_{j,i})$ of Eq. (24) is defined by

$$H(\hat{\Theta}_{j,i}) = \frac{1}{N}\sum_{k=1}^{N}\psi(k,\hat{\Theta}_{j,i})\psi^{T}(k,\hat{\Theta}_{j,i})$$
$$\psi_j(\hat{\Theta}_{j,i}) = \frac{df(\Theta_{j,i})}{d\Theta_{j,i}}\,|_{\Theta_{j,i}=\hat{\Theta}_{j,i}} \tag{25}$$

where $\psi_j(\hat{\Theta}_{j,i})$ is the gradient of the maneuvering model of Eq. (1), and it is specifically defined for each DOF in the following way:

$$\begin{aligned}\psi_{j=1}(\hat{\Theta}_{j=1,i}) &= [\dot{u}\ u\ u|u|]\\ \psi_{j=2}(\hat{\Theta}_{j=2,i}) &= [\dot{v}\ v\ v|v|]\\ \psi_{j=3}(\hat{\Theta}_{j=3,i}) &= [\dot{w}\ w\ w|w|]\\ \psi_{j=4}(\hat{\Theta}_{j=4,i}) &= [\dot{r}\ r\ r|r|]\end{aligned} \tag{26}$$

Additionally, $S_{j,i\ min}$ is determined as follows

$$S_{j,i\ min} = \sqrt{\{H_r^{-1}(\theta_{j,i})\}_{ii}^{-1}} \tag{27}$$

We use as a reference estimator in the present paper the least squares (LS) method, where the aim is to minimize the sum of squared residuals, which is usually denoted as $V(\Theta_{j,i})$. The accuracy and precision of the estimated parameters depend mainly on the model structure and the input signal. The function $V(\Theta_{j,i})$ provides, on the one hand, a measure of the measurement errors of the model signals but, on the other hand, it is also a measure of the errors of its parameters. There is no guarantee that a small value of $V(\Theta_{j,i})$ will provide small errors in the parameter estimates, even in the case that the structure of the model is correct. A necessary but not sufficient condition is that $V(\Theta_{j,i})$ must be sensitive to all parameters. This corresponds to the experiment being rich in information, which requires a persistent excitation signal (Ljung, 1987). The structure of the model must be identifiable. This means that if for a distribution $f(Y_N|\Theta_{j,i})$, there exists more than one value of $f$ that corresponds to a single value of $f$, it is not possible to say which of the two values of $f$ is the correct one, even if the number of samples taken were infinite. In this case, the parameter is said to be unidentifiable (Stuart et al., 1999). The optimization problems proposed in this section attempt to improve this circumstance using the sensitivity metrics mentioned above. In sum, based on the theory stated above, the following steps must be followed to design experiments for the estimation of a non linear maneuvering model of an ROV with model basin tests:

1. Obtain initial parameter estimates $\hat{\Theta}_{j,i}$ close to the optimal parameters estimates with the data acquired in the model basin standard tests, i.e. apply the LS method for the parameter estimation.
2. Choose a preliminary class of physically realizable input signals, i.e. input signals similar to ones used in the standard model basin tests, see Eqs. (16), (17), (18) and (19). The input parameters $\theta_{j,i}$ control the spectrum. For the surge, DOF initializes the input parameters $\theta_{j=1,i}$ by performing an estimation of the second order systems of Eq. (16) which fit the input data acquired in the model basin for the surge DOF and for the sway, heave, and yaw initialize the parameters $\theta_{j=1,i}$, $\theta_{j=2,i}$ and $\theta_{j=3,i}$ by performing an estimation of the parameters of the sinusoidal Eqs. (17), (18) and (19) respectively, which fit the input data acquired in the model basin.
3. Optimize the input signals for the 4 DOF by applying optimization problems of Eq. (14) or (15). Establish tolerances and limits for the input parameters $\theta_{j,i}$ in the cited optimization problems.
4. Check that the obtained input parameters $\theta_{j,i}$, in the convergence of the optimization problems applied in the previous item, provide the best sensitivity values. To do so, calculate and draw some of the characteristic measures of sensitivity as a function of the input signal parameters $\theta_{j,i}$, in the following way:
   - $S_{j,i\ min}$ Eq. (27) as big as possible.
   - $S_{j\ min}$ in Eq. (20) as big as possible.
   - $R_j(\theta_{j,i},\Theta_{j,i})$ Eq. (20)) as close to 1 as possible.
   - $R_{j,i}(\theta_{j,i},\Theta_{j,i}) = S_{j,i\ min}/S_{j\ min}$ as close to 1 as possible.

   if better sensitivity values are found, replace the corresponding input signal parameter $\theta_{j,i}$ in step 3.
5. Use the signal selected in the previous step on the system and obtain improved parameter estimates.
6. If necessary, go back to step 2.

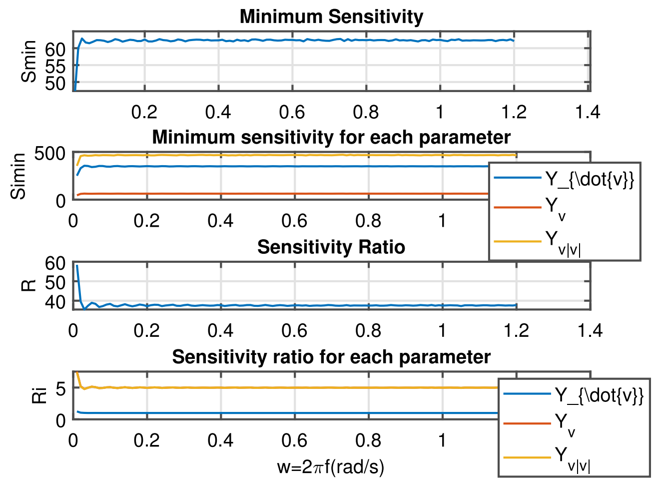


**Fig. 3.** Evolution of the sway sensitivity parameters when $wf$ is varied.

Note that the frequency $w$ of Eqs. (17), (18) and (19) is fixed and was selected in a value close to the frequency of the standard model basin tests. In a preliminary study, it was verified that the variation of the $w$ parameter does not provoke a significant variation in the sensitivity parameters, see Fig. 3 for the sway DOF. Therefore, we have fixed the frequency to the same value as the INTA/CEHIPAR acquired data ($w = 1.047$ rad/s) and varied the amplitudes within limited ranges, as indicated in the previous comment.

It must also be noted that one of the linear regression assumptions of the LS method is that the regressors are not linearly correlated, implying the absence of multicollinearity. The violation of this assumption leads to an inefficient parameter estimation. In the present application, a clear correlation is observed between the linear and non-linear damping terms of the maneuvering model. It is noteworthy that the proposed experiment design methodology does not eliminate the correlation among the cited damping terms, but it has an impact on the efficiency of the parameter estimates. Specifically, the proposed experiment design methodology significantly reduces the variance of the estimated maneuvering parameters, as shown by the Monte Carlo study presented in the case study section.

Additionally, it is important to note that LS estimates for regression models can be sensitive to outliers. Although we have not identified any outliers in the data collected at the INTA/CEHIPAR model basin installations, this remains an important aspect to be considered.

A relationship between the variance of the parameter and the sensitivity of the parameters can be established by applying the Cramer–Rao lower bound:

$$\sigma_{r,\Theta_i} = \sqrt{\frac{2}{N}V(\hat{\Theta}_{j,i})}/S_{i\ min} \tag{28}$$

This result of Eq. (28) is important because the variance is directly proportional to the variance of the noise and inversely proportional to the sensitivity. This means that the higher the sensitivity, the lower the variance of the estimator and the higher the sensitivity, the lower the variance of the estimator, and, therefore, the more efficient the estimator will be.

## 4. Case of study

The experiment design procedure proposed in Section 3 has been applied to the data acquired in the INTA/CEHIPAR installations with the ROV detailed in Appendix. A set of parameters $\hat{\Theta}_{j,i}$ of the maneuvering model has been obtained using LS with standard inputs and the data acquired in the INTA/CEHIPAR installations. We use these estimated parameters as a reference and generate new data contaminated with standard levels of noise of on board instrumentation of ROV when the optimization problems indicated above of Eqs. (14) and (15) are applied. The input signal parameters $\theta_{j,i}$ (Eqs. (17), (18), (19)) have been initialized with the same amplitudes as in the INTA/CEHIPAR multisine inputs for the sway, heave and yaw DOF, see Fig. 2. As far as the surge DOF is concerned, the parameters of three different second-order systems have been estimated through LS, to realistically reproduce the surge input signal used in the INTA/CEHIPAR installations, thus initializing the input parameters $\hat{\theta}_{j=1,i}$ (Eq. (16)). The optimization problems indicated above of Eqs. (14) and (15)are implemented in the Matlab environment with the fmincon and fminimax functions respectively.

As indicated in the experiment design procedure of the previous section, it must be checked that the obtained input parameters $\theta_{j,i}$, when the optimization problem converges, provide the best sensitivity values. This occurs for the sway DOF, which converges at the 40-th iteration for the optimization problem of Eq. (14) and at the 80th iteration for the optimization problem of Eq. (15), see Figs. 6 to 7 for the evolution of the maneuvering model sensitivity parameters. The same is true of the heave DOF, see Figs. 8 and 9 respectively. However, for the yaw and surge DOFs, better sensitivity results are found from previous iterations to the convergence of both optimization problems, Eqs. (14) and (15). Specifically, for the yaw DOF the input parameters at the 8th and 14th iterations for the optimizations problems of Eqs. (14) and (15) respectively, and for the surge DOF at the 10th iteration for both optimization problems. Table 2 compares the sensitivity parameters for the $i$th input parameters iteration previously indicated to the sensitivity parameters of the input data acquired in INTA/CEHIPAR installations for both optimization problems. According to step 4 of the experiment design procedure established in the previous section, an improvement can be observed for most of the sensitivity parameter values for the different DOFs when the standard INTA/CEHIPAR sensitivity parameters are compared to the ones obtained with the proposed optimization problems. In addition, if we compare the sensitivity parameters obtained with the optimization problem of Eq. (14) to the ones obtained with the optimization problem of Eq. (15), similar values are observed for most of the sensitivity parameters.

We develop two different Monte Carlo studies of 100 realizations to verify the improvements of the experiment design compared to the standard input signals with statistical metrics. To do so, a set of parameters of the maneuvering model $\hat{\Theta}_{j,i}$ has been obtained using LS with standard inputs and the data acquired in the INTA/CEHIPAR installations. We use these estimated parameters as a reference and generate new data contaminated with standard levels of noise of on board instrumentation of ROVs. The results of this study are summarized in Tables 3 and 4, where the results given by the standard input are compared to the ones provided with the optimized inputs with a reference OLS estimator. In Table 3, with the optimization problem of Eq. (14), a reduction in bias can be observed for almost all the parameters, except the $N_r$, $N_{r|r|}$ parameters. In the same way, there is a reduction in variance for almost all the parameters, except for the $N_r$, $N_{r|r|}$, $N_{\dot{r}}$ parameters. Furthermore, Table 4, with the optimization problem of Eq. (15), shows with the optimized input a reduction in bias, with the only exception of the $Y_{v|v|}$ parameter and a reduction in variance except for the $N_r$ parameters. In both optimization problems, it can be concluded that the optimized inputs provide more accurate and efficient parameter estimates than with the standard INTA/CEHIPAR inputs using OLS as a reference estimator. Moreover, the results with

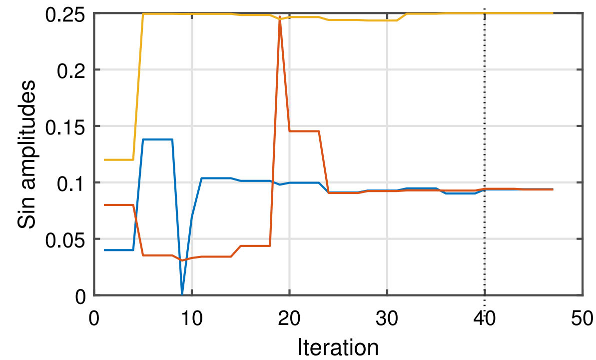


**Fig. 4.** Convergence of the amplitudes for the sway multisin input signal, optimization problem of Eq. (14).

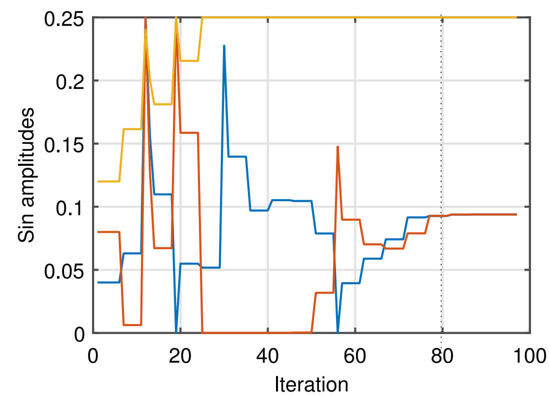


**Fig. 5.** Convergence of the amplitudes for the sway multisin input signal, optimization problem of Eq. (15).

the optimizations problem of Eq. (15) present fewer exceptions in bias and variance reduction; therefore, it is chosen as the better option. Fig. 14, shows the experiment design results with the optimizations problem of Eq. (15). If we compare this figure to the standard inputs of Fig. 2, apart from the cited parameter estimation results, there is a significant reduction in the time interval with the proposed experiment design, which constitutes a considerable reduction of the model basin tests costs. In addition, Fig. 14 compares the INTA/CEHIPAR acquired data to the experiment design results for the surge DOF. Since the optimized input signal for the surge DOF has more possibilities of abrupt accelerations, it is important to note that the first two changes in the experiment design results are of similar levels to the acquired data, while the third change in the experiment design presents an acceleration peak much higher but not excessive. Nonetheless, it is possible to adjust the rise time in case of overcoming the carriage acceleration system for a specific installation since for the surge DOF, the input signal is established as a second-order system in Eq. (16) (see Figs. 4, 5, 10–13 and 15).

## 5. Conclusions

In the present paper, we propose an experiment design methodology based on a parameter sensitivity approach for the parameter estimation of non-linear maneuvering models of ROVs. The experiment design methodology is applied to the model basin tests performed in the INTA/CHEIPAR installation where the input signals used are constrained to the dimensions of the cited installations. Two different optimization problems in the application of the experiment design methodology are compared and the one which provides the best results is selected. The results show considerable improvements in all

**Table 2**
Comparative table with sensitivity parameter results for the standard input and the inputs designed with the optimization problems of Eqs. (14) and (15).

| Input | Sensitivity | Surge | Sway | Heave | Yaw |
|---|---|---|---|---|---|
| Standard | $S_{min}$ | 4.88 | 0.150285 | 1.02 | 2.81 |
| | $S_{i\ min}$ | 15.6 4.8 25.8 | 1.8 1.2 0.34 | 49.5 3.43 3.59 | 5.9 12.87 15.63 |
| | $R_i$ | 4.4 1.0 4.4 | 3.2 1 3.2 | 3.4 1.0 3.48 | 1 3.56 3.56 |
| | $R$ | 27.38 | 17.7 | 48.3 | 7.13 |
| Designed, Eq. (14) | $S_{min}$ | 1.37 | 3.25 | 3.9 | 3.6 |
| | $S_{i\ min}$ | 1.37 111.2 345.6 | 20.3 18.2 10.8 | 34.2 17.4 14.8 | 5.9 12.7 20,2 |
| | $R_i$ | 1 4.4 4.4 | 1 2.9 2.9 | 1 2.9 2.9 | 1 3 3 |
| | $R$ | 262.6 | 6.45 | 8.6 | 6.5 |
| Designed, Eq. (15) | $S_{min}$ | 1.38 | 3.24 | 2.98 | 4.19 |
| | $S_{i\ min}$ | 1.37 110.27 346.4 | 20.3 18.2 10.8 | 42.9 21.7 20.6 | 8.7 18.8 38.7 |
| | $R_i$ | 1 5 5 | 1 2.9 2.9 | 1 5 5 | 1 4 4 |
| | $R$ | 263,3 | 6.45 | 14 | 10.2 |

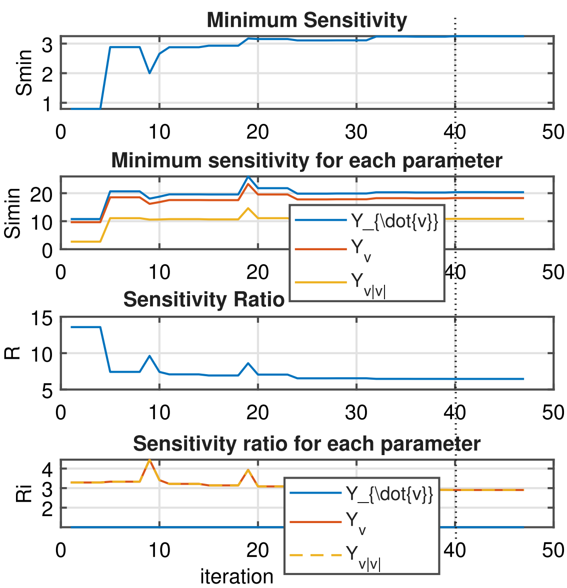


**Fig. 6.** Evolution of the sway sensitivity parameters for the optimization problem of Eq. (14).

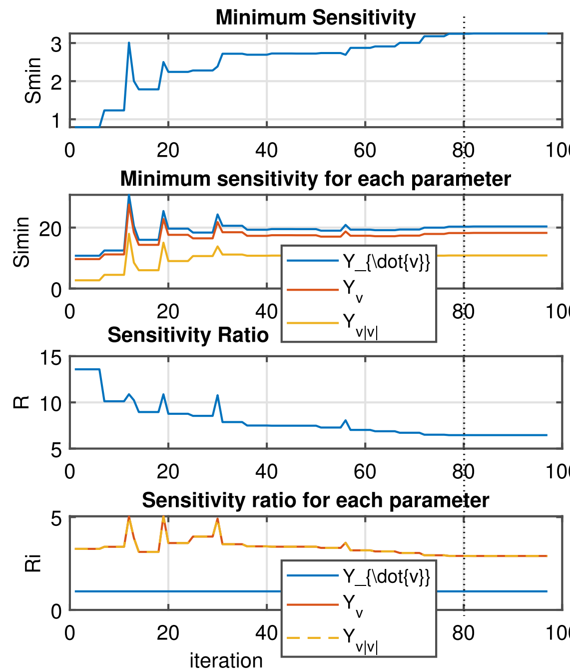


**Fig. 7.** Evolution of the sway sensitivity parameters for the optimization problem of Eq. (15).

**Table 3**
Monte Carlo study of 100 realizations comparing standard INTA/CEHIPAR inputs to the ones obtained with the optimization problem of Eq. (14).

| | Standard input | | Min input | |
|---|---|---|---|---|
| | Bias | Std. dev. | Bias | Std. dev. |
| $X_{\dot{u}}$ | 0.1994 | 3.0631 | 0.0336 | 1.7568 |
| $X_u$ | 0.0008 | 0.0294 | 0.0007 | 0.0274 |
| $X_{u\|u\|}$ | 0.0008 | 0.0223 | 0.0002 | 0.0160 |
| $Y_{\dot{v}}$ | 0.0171 | 0.1503 | 0.0010 | 0.0860 |
| $Y_v$ | 0.0319 | 0.5373 | 0.0278 | 0.2612 |
| $Y_{v\|v\|}$ | 0.5410 | 5.8766 | 0.1678 | 1.3403 |
| $Z_{\dot{w}}$ | 0.0170 | 0.3128 | 0.0053 | 0.0082 |
| $Z_w$ | 0.1126 | 1.0867 | 0.0418 | 0.2925 |
| $Z_{w\|w\|}$ | 1.9161 | 20.4460 | 0.1855 | 1.4862 |
| $N_{\dot{r}}$ | 0.0043 | 0.0509 | 0.0006 | 0.0883 |
| $N_r$ | 0.0086 | 0.1873 | 0.0184 | 0.6289 |
| $N_{r\|r\|}$ | 0.0033 | 0.7102 | 0.0107 | 1.6289 |

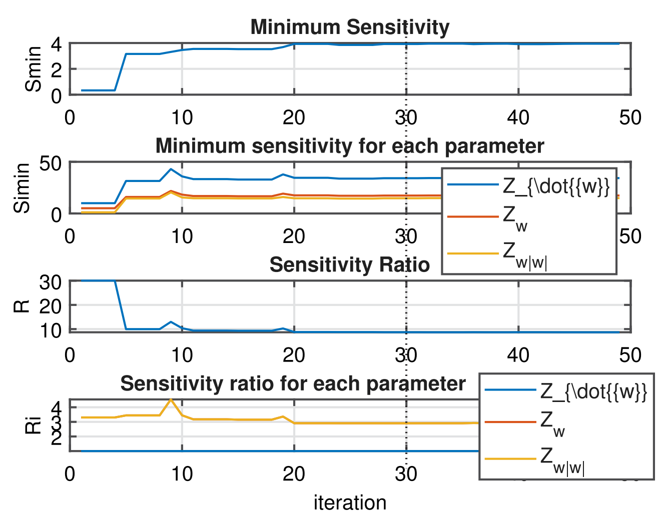


**Fig. 8.** Evolution of the heave sensitivity parameters for the optimization problem of Eq. (14).

the sensitivity parameters, when the standard INTA/CEHIPAR input sensitivity parameters are compared to the ones obtained with the proposed experiment design methodology. Moreover, the Monte Carlo study results exhibit a reduction in bias and variance for almost all the parameters, making it possible to conclude that the optimized

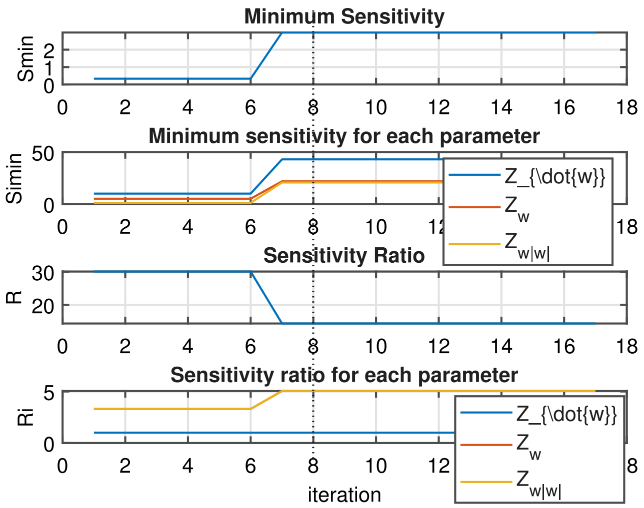


Fig. 9. Evolution of the heave sensitivity parameters for the optimization problem of Eq. (15).

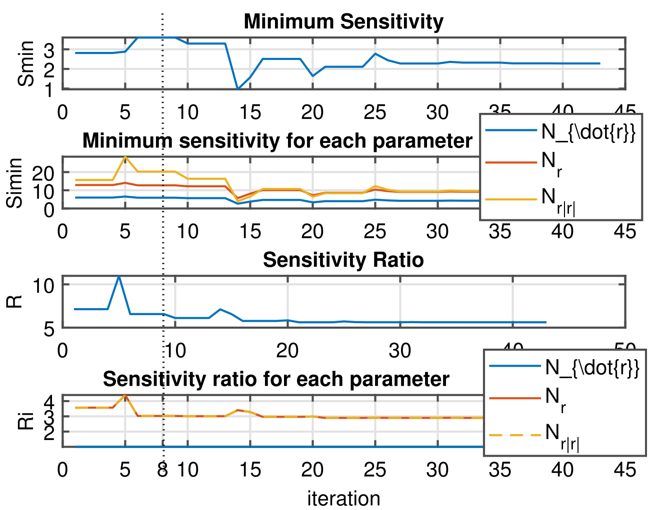


Fig. 10. Evolution of the yaw sensitivity parameters for the optimization problem of Eq. (14).

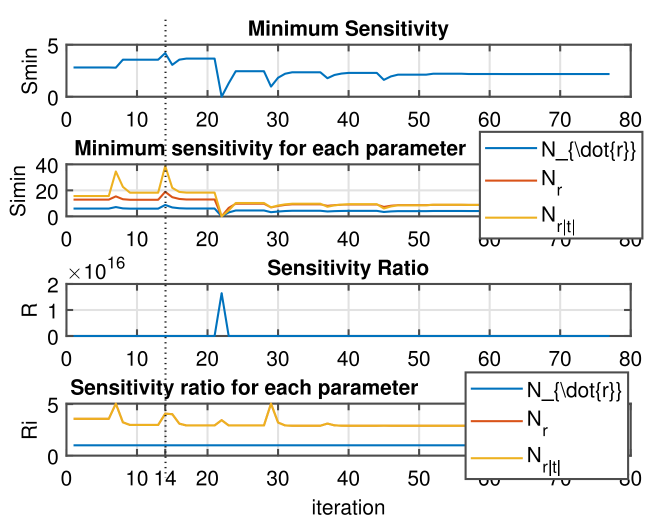


Fig. 11. Evolution of the yaw sensitivity parameters for the optimization problem of Eq. (15).

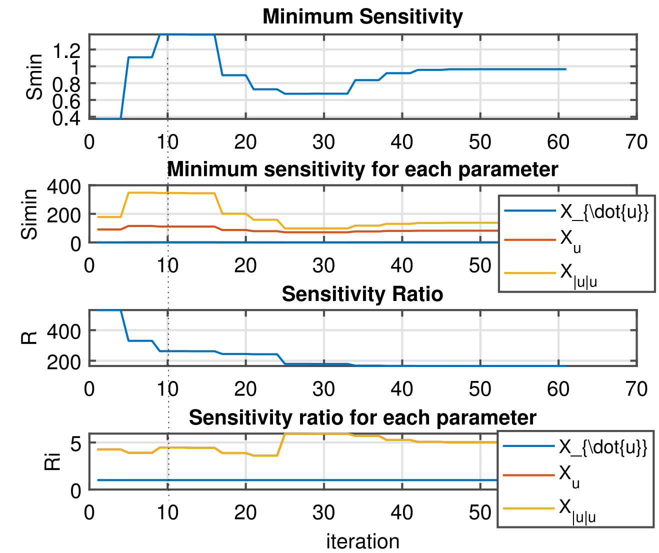


Fig. 12. Evolution of the surge sensitivity parameters for the optimization problem of Eq. (14).

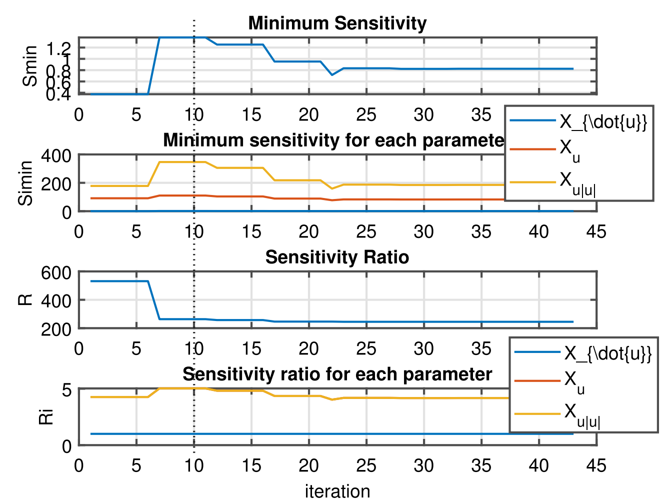


Fig. 13. Evolution of the surge sensitivity parameters for the optimization problem of Eq. (15).

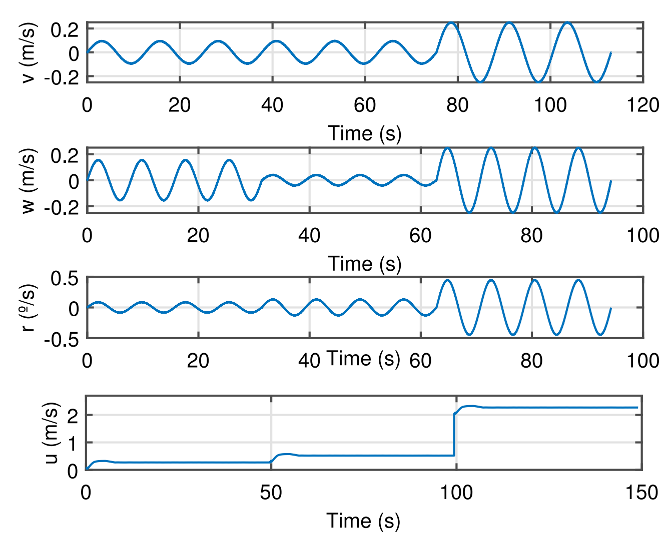


Fig. 14. Experiment design results for the sway, heave, yaw and surge DOFs.

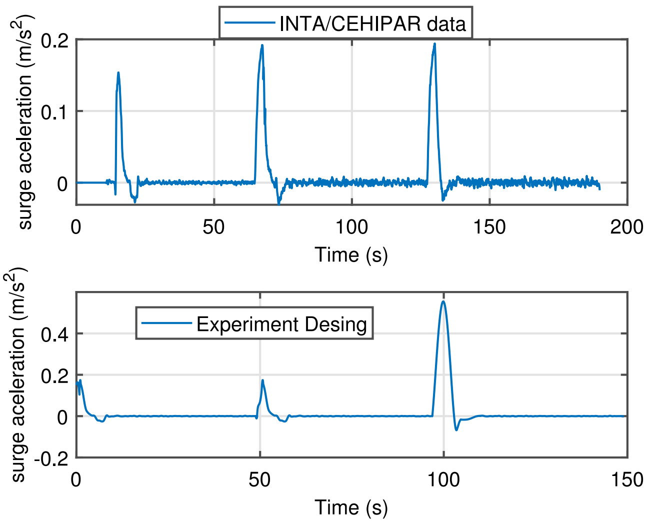


**Fig. 15.** Comparing the INTA/CEHIPAR data to the Experiment design results for surge DOF.

**Table 4**
Monte Carlo study of 100 realizations comparing standard INTA/CEHIPAR inputs to the ones obtained with the optimization problem of Eq. (15).

| | Standard input | | Min input | |
|---|---|---|---|---|
| | Bias | Std. dev. | Bias | Std. dev. |
| $X_{\dot{u}}$ | 0.5077 | 3.2830 | 0.0508 | 0.8767 |
| $X_u$ | 0.0041 | 0.0335 | 0.0015 | 0.0338 |
| $X_{u\|u\|}$ | 0.0028 | 0.0244 | 0.0007 | 0.0150 |
| $Y_{\dot{v}}$ | 0.0083 | 0.1594 | 0.0067 | 0.0733 |
| $Y_v$ | 0.0304 | 0.5379 | 0.0142 | 0.2481 |
| $Y_{v\|v\|}$ | 0.3542 | 5.7282 | 0.0487 | 1.2919 |
| $Z_{\dot{w}}$ | 0.0670 | 0.2890 | 0.0144 | 0.0750 |
| $Z_w$ | 0.0353 | 1.0066 | 0.0238 | 0.3652 |
| $Z_{w\|w\|}$ | 0.5098 | 19.0148 | 0.1347 | 1.7446 |
| $N_{\dot{r}}$ | 0.0067 | 0.0554 | 0.0037 | 0.0507 |
| $N_r$ | 0.0202 | 0.1860 | 0.0182 | 0.1877 |
| $N_{r\|r\|}$ | 0.0831 | 0.7399 | 0.0594 | 0.5980 |

**Table 5**
ROV main data.

| | Value | Description |
|---|---|---|
| $m$ (kg) | 80.750 | total mass |
| $x_G$ (m) | 0.490 | Distance in the $X$ axis from the CG to $O_b$ |
| $z_G$ (m) | 0.400 | Distance in the $Z$ axis from the CG to $O_b$ |
| $I_{xx}$ (Kgm$^2$) | 0.29 | Inertia roll |
| $I_{yy}$ (Kgm$^2$) | 6.945 | Inertia pitch |
| $I_r$ (Kgm$^2$) | 7.073 | Inertia yaw |

inputs provide more accurate and efficient parameter estimates than with the standard INTA/CEHIPAR inputs using OLS as a reference estimator. The optimizations problem of Eq. (15) is selected as the best option, since the results present less exceptions in bias and variance reduction. In addition, the experiment design methodology with the selected optimization problem also provides a significant reduction in the time interval with respect to the standard INTA/CHEIPAR input signals, which constitutes a considerable reduction of the model basin tests costs. In subsequent research, this experiment design procedure could be applied with another estimator for further improvements.

## CRediT authorship contribution statement

**Elías Revestido Herrero:** Writing – original draft, Validation, Methodology, Investigation. **Jose Ramon Llata:** Methodology, Investigation. **Jose Joaquin Sainz:** Writing – review & editing, Methodology. **Francisco J. Velasco:** Project administration. **Luciano Alonso Renteria:** Software.

**Table 6**
Maneuvering model parameters.

| | Parameters | Equation |
|---|---|---|
| $X_{\dot{u}}$ | −156.239 | |
| $X_u$ | −81.5 | (10) |
| $X_{u\|u\|}$ | −116.325 | |
| $Y_{\dot{v}}$ | −157.6 | |
| $Y_v$ | −175.43 | (12) |
| $Y_{v\|v\|}$ | −483.5 | |
| $Z_{\dot{w}}$ | −295.8 | |
| $Z_w$ | −152,4 | (11) |
| $Z_{w\|w\|}$ | −660.7 | |
| $N_{\dot{r}}$ | −30.7 | |
| $N_r$ | −69.1 | (13) |
| $N_{r\|r\|}$ | −322.3 | |

## Declaration of competing interest

The authors declare that they have no known competing financial interests or personal relationships that could have appeared to influence the work reported in this paper.

## Data availability

The authors do not have permission to share data.

## Acknowledgments

This project has been partially supported through the project TED2021-132158B-I00 Evolutionary Monitoring with Unmanned Underwater Vehicles for the Maintenance of the bottom and Anchorages of Offshore Wind Farms funded by MCIU/AEI/10.13039/501100011033 and by the European Union - Next GenerationEU/PRTR (Fig. 16) and through the proyect Control of Unmanned Underwater Vehicles for Supervision of Structures for Anchored Maritime Works. Advanced and Inteligent Controllers & 3D Supervision funded by the Ministry Of Universities, Equality, Culture and Sport of The Government of Cantabria, Spain.

## Appendix. Experimental set up and ROV main features

The experimental setup used for the model basin tests is depicted in Fig. 17. The figure shows the positions of the actuators along with their distances to the center of gravity (CG). The submerged depth for the trials was chosen to be 1.2 m from the water surface up to the top face of the ROV. This selection was based on preliminary CFD calculations, which indicated that the free surface effects of the water were negligible at the immersion depth of 1 m.

The ROV is shown in Fig. 18, its dimensions are 1 m × 0.6 m, 0.62 m. The moments of inertia, the center of gravity, and the center of buoyancy of the vehicle are found in Table 5. The center of gravity and inertia of the ROV were obtained experimentally by forced oscillations. The values obtained are shown in Table 1. In this vehicle, four thrusters in x-type are mounted for the surge, sway, and yaw motion, and a vertical one for depth control. The set of parameters $\hat{\Theta}_{j,i}$ of the maneuvering model used as a reference to generate new data contaminated with standard levels of noise of on board instrumentation of the ROV in Fig. 18 when the optimization problems indicated above (Eqs. (14) and (15)) are applied can be found in Table 6.

**Fig. 16.** MCIU/ AEI /10.13039/501100011033 and the European Union - Next GenerationEU/PRTR.

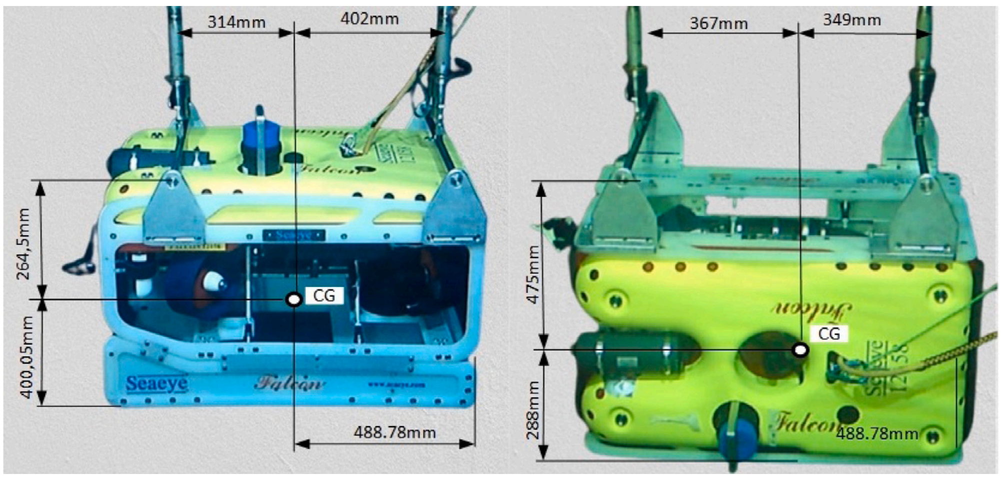


**Fig. 17.** ROV assemblies set up in the INTA/CEHIPAR calm water channel, right upright position and left ROV turned 90 degrees.

**Fig. 18.** ROV and inertial table for the inertias obtention.

## References

Alabsi, M., Fields, T., 2019. Quadrotor aircraft intelligent system identification experiment design. Proc Inst. Mech. Eng. G(J. Aerosp. Eng.) 233 (13), 4911–4925. http://dx.doi.org/10.1177/0954410019833209.

Barker, H., Rivera, D., Tan, A., Godfrey, K., 2006. Perturbation signal design. In: IFAC Symposium Modelling, Identification and Signal Processing (SYSID 2006) Identification and System Parameter Estimation. p. 6.

Beelen, H., Bergveld, H., Donkers, M., 2018. On experiment design for parameter estimation of equivalent-circuit battery models. In: 2018 IEEE Conference on Control Technology and Applications. CCTA, pp. 1526–1531. http://dx.doi.org/10.1109/CCTA.2018.8511529, battery management;lithium-ion batteries;equivalent-circuit battery models;battery management;model-based state estimation techniques;E-bike;parameter estimation;experiment design;ECM parameters;state estimate;accurate model parameters;Li;.

Blanke, M., Knudsen, M., 1999. Optimized experiment design for marine systems identification. In: Proceedings of the 14th World Congress. International Federation of Automatic Control, vol. 17, Kidlington, UK, pp. 575–580.

Blanke, M., Knudsen, M., 2006. Efficient parameterization for grey-box model identification of complex physical systems. In: IFAC Symposium Modelling, Identification and Signal Processing (SYSID 2006) Identification and System Parameter Estimation. Amsterdam, Netherlands, p. 6.

Bombois, X., Morelli, F., Hjalmarsson, H., Bako, L., Colin, K., 2021. Robust optimal identification experiment design for multisine excitation. Automatica 125, 109431. http://dx.doi.org/10.1016/j.automatica.2020.109431, URL: https://www.sciencedirect.com/science/article/pii/S0005109820306336.

Braun, M., Rivera, D., Stenman, A., 2001. A model-on-demand identification methodology for non-linear process systems. Internat. J. Control 74 (18), 1708–1717.

Capocci, R., Dooly, G., Omerdic, E., Coleman, J., Newe, T., Toal, D., 2017. Dictionary-based experiment design for estimation of marine models. J. Mar. Sci. Eng. 5 (1), http://dx.doi.org/10.3390/jmse5010013, 13 (32 pp.).

Committee, M., 2014. Final Report and Recommendations to the 27 th ITTC. Technical Report, 27th ITTC Copenhagen.

Denis-Vidal, L., Jauberthie, C., Kieffer, M., 2019. Optimal experiment design for bounded-error estimation of nonlinear models. In: 2019 IEEE 58th Conference on Decision and Control. CDC, pp. 4147–4154. http://dx.doi.org/10.1109/CDC40024.2019.9030003.

Denisov, V., Chubich, V., Filippova, E., 2019. The optimal estimation of parameters of models of controlled stochastic systems based on the experiment design. 1333, http://dx.doi.org/10.1088/1742-6596/1333/3/032020, 032020 (7 pp.),

Dirkx, N., Tiels, K., Oomen, T., 2023. Iterative robust experiment design for MIMO system identification via the S-lemma. In: 2023 IEEE Conference on Control Technology and Applications. CCTA, pp. 998–1003. http://dx.doi.org/10.1109/CCTA54093.2023.10252362.

Du, X., Engelmann, A., Jiang, Y., Faulwasser, T., Houska, B., 2019. Optimal experiment design for AC power systems admittance estimation. p. 6, arXiv.

Fay, D., Stanton, N., Roberts, A., 2019. Exploring ecological interface design for future ROV capabilities in maritime command and control. In: Advances in Human Aspects of Transportation. Proceedings of the AHFE 2018 International Conference on Human Factors in Transportation. Advances in Intelligent Systems and Computing. AISC 786, pp. 264–273. http://dx.doi.org/10.1007/978-3-319-93885-1_24.

Fossen, T., 2002. Marine Control Systems: Guidance, Navigation and Control of Ships, Rigs and Underwater Vehicles. Marine Cybernetics.

Fossen, T.I., 2011. Handbook of Marine Craft Hydrodynamics and Motion Control. John Wiley and Sons, Ltd, arXiv:https://onlinelibrary.wiley.com/doi/pdf/10.1002/9781119994138.fmatter, URL: https://onlinelibrary.wiley.com/doi/abs/10.1002/9781119994138.fmatter.

Fredrik Ljungberg, M.E., Tervo, K., 2023. Dictionary-based experiment design for estimation of marine models. Control Eng. Pract. 135, 105528. http://dx.doi.org/10.1016/j.conengprac.2023.105528, URL: https://www.sciencedirect.com/science/article/pii/S0967066123000977.

Goodwin, G., Payne, R., 1977. In: Mathematics and Science Engineering (Ed.), Dynamic System Identification: Experiment Design and Data Analysis.

Gopaluni, R.B., Schön, T.B., Wills, A.G., 2009. Particle filter approach to nonlinear system identification under missing observations with a real application. IFAC Proc. Vol. 42, 810–815.

Gottu Mukkula, A., Paulen, R., 2019. Optimal experiment design in nonlinear parameter estimation with exact confidence regions. J. Process Control 83, 187–195. http://dx.doi.org/10.1016/j.jprocont.2019.01.004.

Herrero, E.R., Gonzalez, F.J.V., García, E.L., Perez, E.M., 2012. Diseño de Experimentos para la Estimación de Parámetros de Modelos de Maniobra Lineales de Buques. Revista Iberoamericana de Automética e Informética Industrial RIAI 9 (2), 123–134. http://dx.doi.org/10.1016/j.riai.2012.02.006, URL: https://www.sciencedirect.com/science/article/pii/S1697791212000076.

Lee, S.-K., Joung, T.-H., Cheo, S.-J., Jang, T.-S., Lee, J.-H., 2011. Evaluation of the added mass for a spheroid-type unmanned underwater vehicle by vertical planar motion mechanism test. Int. J. Nav. Archit. Ocean Eng. 3 (3), 174–180. http://dx.doi.org/10.2478/IJNAOE-2013-0060, URL: http://www.sciencedirect.com/science/article/pii/S2092678216302205.

Ljung, L., 1987. System Identification: Theory for the User. Prentice-Hall.

McMichael, R.D., Blakley, S.M., 2022. Simplified algorithms for adaptive experiment design in parameter estimation. Phys. Rev. A 18, 054001. http://dx.doi.org/10.1103/PhysRevApplied.18.054001, URL: https://link.aps.org/doi/10.1103/PhysRevApplied.18.054001.

Pérez, T., Fossen, T., 2006. Time-domain models of marine surface vessels based on seakeeping computations. In: Proc. 7th IFAC Conference on Manoeuvring and Control of Marine Craft MCMC. Lisbon, Portugal.

Phillips, A., Furlong, M., Turnock, S., 2007. Virtual planar motion mechanism tests of the autonomous underwater vehicle autosub. In: STG-Conference / Lectureday "CFD in Ship Design". Institute M-8 of Hamburg University of Technology, URL: http://eprints.soton.ac.uk/48939/.

Revestido Herrero, E., Velasco, F.J., Riola Rodríguez, J.M., 2018. Improving parameter estimation efficiency of a non linear manoeuvring model of an underwater vehicle based on model basin data. Appl. Ocean Res. 76, 125–138. http://dx.doi.org/10.1016/j.apor.2018.04.012, URL: https://www.sciencedirect.com/science/article/pii/S0141118717304406.

Robert L. Wernli, R.D.C., 2014. The ROV Manual (Second Edition), second ed. In: A User Guide for Remotely Operated Vehicles, Butterworth-Heinemann, pp. i–iii. http://dx.doi.org/10.1016/B978-0-08-098288-5.00024-5, URL: https://www.sciencedirect.com/science/article/pii/B9780080982885000245.

Rojas, C.R., Aguero, J.-C., Welsh, J.S., Goodwin, G.C., Feuer, A., 2012. Robustness in experiment design. IEEE Trans. Autom. Control 57 (4), 860–874. http://dx.doi.org/10.1109/TAC.2011.2166294.

Schjlberg, I., Utne, I.B., 2015. Towards autonomy in ROV operations. IFAC-PapersOnLine 48 (2), 183–188. http://dx.doi.org/10.1016/j.ifacol.2015.06.030, URL: https://www.sciencedirect.com/science/article/pii/S2405896315002694, 4th IFAC Workshop onNavigation, Guidance and Controlof Underwater VehiclesNGCUV 2015.

Shen, C., Buckham, B., Shi, Y., 2017. Modified c/GMRES algorithm for fast nonlinear model predictive tracking control of AUVs. IEEE Trans. Control Syst. Technol. 25 (5), 1896–1904. http://dx.doi.org/10.1109/TCST.2016.2628803.

Söderström, T., Stoica, P., 1994. System Identification. Prentice-Hall.

Soylu, S., Proctor, A.A., Podhorodeski, R.P., Bradley, C., Buckham, B.J., 2016. Precise trajectory control for an inspection class ROV. Ocean Eng. 111, 508–523. http://dx.doi.org/10.1016/j.oceaneng.2015.08.061.

Stuart, A., Ord, K., Arnold, S., 1999. Classical inference and the linear model, sixth ed. In: Kendal's Advanced Theory of Statistics, vol. 2A, Arnold.

Valenzuela, P.E., Dahlin, J., Rojas, C.R., Schön, T.B., 2014. A graph/particle-based method for experiment design in nonlinear systems. IFAC Proc. Vol. 47 (3), 1404–1409. http://dx.doi.org/10.3182/20140824-6-ZA-1003.00361, URL: https://www.sciencedirect.com/science/article/pii/S1474667016418094, 19th IFAC World Congress.

Valenzuela, P.E., Rojas, C.R., Hjalmarsson, H., 2013. Optimal input design for non-linear dynamic systems: A graph theory approach. arXiv:1310.4706.

Zimmermann, S., Enqvist, M., Gunnarsson, S., Moberg, S., Norrlof, M., 2023. Experimental evaluation of a method for improving experiment design in robot identification. In: 2023 IEEE International Conference on Robotics and Automation. ICRA, pp. 11432–11438. http://dx.doi.org/10.1109/ICRA48891.2023.10161092.